Optical Materials 138 (2023) 113618

Contents lists available at ScienceDirect

Optical Materials

journal homepage: www.elsevier.com/locate/optmat

Research article

High-efficiency silicon metasurface mirror on a sapphire substrate

Mariia Matiushechkina [a,c,*], Andrey B. Evlyukhin [b,c,**], Vladimir A. Zenin [d], Michèle Heurs [a,c], Boris N. Chichkov [b,c]

[a] Institute for Gravitational Physics, Leibniz University Hannover, Callinstr. 38, Hannover 30167, Germany
[b] Institute of Quantum Optics, Leibniz University Hannover, Welfengarten 1, Hannover 30167, Germany
[c] Cluster of Excellence PhoenixD, Leibniz University Hannover, Welfengarten 1A, Hannover 30167, Germany
[d] Center for Nano Optics, University of Southern Denmark, Campusvej 55, Odense 5230, Denmark

ARTICLE INFO

Keywords:
Metasurface
Silicon nano-coating for telecom wavelength
Optics in gravitational wave interferometers

ABSTRACT

For a possible implementation of high-efficiency Si-nanosphere metasurface mirrors functioning at telecom wavelengths in future gravitational wave detectors, exact dimensional and configuration parameters of the total system, including substrate and protective coating, have to be determined a priori. The reflectivity of such multi-layer metasurfaces with embedded Si nanoparticles and their potential limitations need to be investigated. Here we present the results on how the substrate and protective layer influence optical properties and demonstrate how dimensional and material characteristics of the structure alter light reflectivity. Additionally, we consider the impact of manufacturing imperfections, such as fluctuations of Si nanoparticle sizes and their exact placement, on the metasurface reflectivity. Finally, we demonstrate how high reflectivity of the system can be preserved under variations of the protective layer thickness, incident angle of light, and its polarization.

1. Introduction

Investigations of resonant optical properties of silicon nanoparticles have received significant attention during the last decade [1–4]. Due to the high refractive index, silicon nanoparticles can support electric and magnetic types of multipole resonances [5]. It is important to note that the respective spectral positions of the electric and magnetic multipole resonances can be controlled by specifying the particle shape, irradiation conditions, or by arranging the nanoparticles into special periodic structures [6–8]. In these cases, excitation of different multipole resonances and their overlap in specified spectral ranges can be used to monitor and control the process of light scattering, including its intensity and radiation pattern. These possibilities provide interesting applications of silicon nanoparticles for the realization of compact optical devices with tailored functional properties. It has been shown that by using 2D arrays of disk-like silicon nanoparticles it is possible to make Huygens metasurfaces [9,10]. Such metasurfaces exhibit total transmission at resonant conditions due to interference between the scattered fields generated by the resonant electric and magnetic dipole moments of nanoparticles. A similar effect (full resonant transmission) can be realized in metasurfaces consisting of spherical silicon nanoparticles [11]. The effect of full reflectance is observed when the structure is tuned only to one of the dipole resonances [12]. Destructive interference between the scattered and incident light fields prevents the beam from propagating through the structure, and so due to energy conservation, the total light field is reflected back. Using this property of high-reflectivity and varying the combinations of materials and geometric parameters, the technology is improving in areas such as wireless telecommunication, wavefront manipulation and high-quality imaging [13–16].

Crystalline silicon has a negligibly weak light absorption in the near infrared range. For this reason, metasurfaces of silicon nanoparticles have been proposed for the implementation of highly efficient optical mirrors [17]. It has been shown that periodic arrays of spherical silicon nanoparticles can demonstrate full suppression of light transmission and provide almost 100% reflection at the resonant electric or magnetic dipole conditions. In recent publications [18,19] it has been shown how an array of silicon nanospheres in a homogeneous medium can act as a high-reflective mirror at specified wavelengths. Such mirrors have a range of advantageous characteristics (e.g., ultra-compact, lightweight, and robust) that make them very attractive for precision metrology and specialized applications. In particular, these mirrors can be used in the field of modern quantum optics as a part of an optical cavity, a photodetector or other devices [20–22]. Moreover, their potential suitability is currently being investigated as an alternative high-reflective

* Corresponding author at: Institute for Gravitational Physics, Leibniz University Hannover, Callinstr. 38, Hannover 30167, Germany.
** Corresponding author.
E-mail addresses: mariia.matiushechkina@aei.mpg.de (M. Matiushechkina), a.b.evlyukhin@daad-alumni.de (A.B. Evlyukhin).

https://doi.org/10.1016/j.optmat.2023.113618
Received 9 November 2022; Received in revised form 16 February 2023; Accepted 19 February 2023
Available online 2 March 2023

coating for mirrors in next-generation interferometric gravitational wave observatories.

With the potential laser beam operation wavelength of 1550 nm, the cavity optics of the gravitational wave interferometers will be made from the materials like sapphire or silicon [23,24]. The choice of coating is still under discussion. The requirements to be fulfilled are low optical and mechanical losses. The reflectance for different mirrors can vary in the range of absolute to partial reflection. Current dielectric coatings have excellent optical and extremely good mechanical properties. However, the internal friction between the layers of different amorphous oxides, in combination with the thermal noise from each individual layer, generates one of the limiting displacement noises [25–27]. Moreover, the thickness of such coatings is in the range of 2 to 6 micrometers. We propose an alternative idea of using a metastructure, in particular a metasurface, as a coating for the optics in future gravitational wave detectors. The metasurface has several advantages: The thickness of the structure is on the nanometer scale. Moreover, high reflectance is achieved by using only one layer of nanoparticles avoiding contact between several different material layers and therefore promising lower mechanical loss.

This article reports on our work towards the development of silicon nanosphere metasurface mirror at 1550 nm wavelength for potential implementation in next-generation gravitational wave detectors. Building on our previous studies that demonstrated the absolute 100% reflection at a single wavelength of the metasurfaces located in a homogeneous and isotropic environment [19], in this article we investigate the influence of multi-layer inhomogeneous media, including substrate and protective coating, on the reflective properties of the metasurfaces. With the knowledge that the substrate material below and a material layer in-between the nanoparticle array can change the optical properties of the whole structure [28–32], we perform a detailed numerical analysis of the induced effects. The proposed design of the metasurface is taken as a periodic construction of silicon nanospheres placed on a sapphire substrate and embedded in a protective layer (PL) with a certain refractive index. We demonstrate that the presence of the sapphire substrate does not deteriorate high reflection of light from the metasurface at a fixed wavelength; however, the protective layer shifts the parameters of perfect resonant condition and therefore, has to be taken into account before the fabrication process. Detailed modeling is performed to determine the optimum dimensional parameters of the metasurface that provide high reflection of light at the wavelength of 1550 nm. Moreover, we test the robustness of the metasurface mirror to possible imperfections (deviations in the size of nanoparticles and their positions).

2. Model of the structure and physical description

2.1. Main parameters and configuration

The geometrical configuration of the structure is presented in Fig. 1 as an array of nanospheres placed on a sapphire substrate. The spheres have a fixed diameter (D) and are placed at equal distances from each other (periodicity P). They touch the substrate only at one point and can be embedded in an additional protective layer with thickness (h).

The choice of materials is motivated by the chosen wavelength of 1550 nm of the incident light, which is considered to be a linearly polarized plane wave incident perpendicular to the structure. Considering optical and mechanical properties, we selected Si as a high refractive index material for the realization of the nanoparticle array. Note that for Si, the absorption of infrared light at wavelengths around 1550 nm is negligible. Sapphire was chosen as the substrate material as one of the material candidates for use in gravitational wave detectors. In contrast to Si, sapphire has low refractive index and therefore has less impact on the metasurface behavior. A suitable material for the embedding protective layer (PL) is still under discussion. However, the necessity of using of such a layer is obvious, as the nanostructure needs

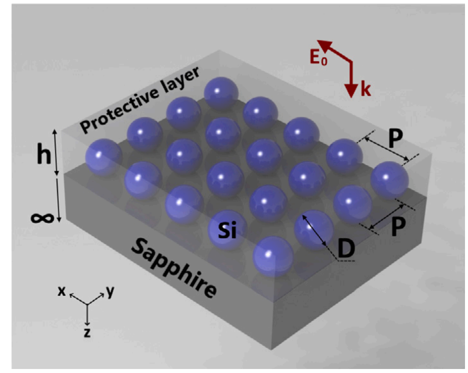

Fig. 1. Schematic view of silicon nanospheres forming a periodic structure (metasurface) on top of a sapphire substrate, embedded in a protective layer. Each nanosphere has a fixed diameter (D) and is placed with distance P (periodicity) in x- and y-directions to the neighboring spheres. The metasurface is irradiated by a plane monochromatic light wave under normal incidence with respect to the metasurface plane: $\mathbf{E}_0$ and $\mathbf{k}$ are the electric field and the wave vector, respectively.

to be shielded from any kind of damage. The minimum requirement is that it should have minimal absorption (i.e. be relatively transparent) for the light, and that its contribution to the mechanical noise should be low. One of the prospective materials to be used is fused silica with a refractive index of 1.4 at 1550 nm wavelength. In order to implement a metasurface mirror in future gravitational wave detectors, all of the materials of the mirror should exhibit high mechanical quality factor. The mechanical quality factor of sapphire is higher than 10^9 [33]. For silicon, a significant reduction of thermo-elastic noise and consequently a high mechanical quality factor have been demonstrated at temperatures of 123 K and 18 K [34]. In this article, the operation of the modeled nanostructure is considered at room temperature.

2.2. Numerical approach

The fundamental behavior of a metasurface is based on the process of Mie-scattering [35]. The theoretical description and calculation approaches for the silicon metasurface mirror in a homogeneous PDMS layer were discussed here [19]. In this article, we get closer to the realistic case, where we consider Si nanoparticles on a sapphire substrate embedded in an additional layer to protect the nanostructure from mechanical damage. The theoretical interpretation of the multiple medium model is more complicated due to the additional transmission and reflection terms induced by the Fabry–Perot effect in the sapphire substrate and the embedding layer, which are responsible for the alteration of the results for the nanoparticle structure in a homogeneous surrounding. At the same time, the physical origin of optical reflectance is still based on Mie-scattering. To model the nanostructure and to simulate its behavior under various geometrical and material parameters, including imperfection effects, we use the commercial simulation software COMSOL Multiphysics. The computational process is based on the finite element method, which allows for analysis of the system with multiple modifications. The configuration, size, material parameters and irradiation conditions used in numerical simulations are indicated in this subsection and 2.1. Parameters for imperfection simulations are provided in the following Section 3.2.

First of all, we investigate the array of Si nanoparticles (refractive index $n_{\mathrm{Si}} = 3.48$) located in air and placed on a sapphire substrate ($n_{\mathrm{sub}} = 1.75$). Secondly, we study the case when this nanoparticle array is embedded in a protective layer (refractive index $n_{\mathrm{PL}} = 1.4$) with the thickness equal to the nanoparticle diameter. Fig. 2 shows the intensity reflection coefficients calculated as a function of the nanoparticle diameter (D) and the array periodicity (P) for both cases and for a normal incident plane wave with the wavelength of 1550 nm. The

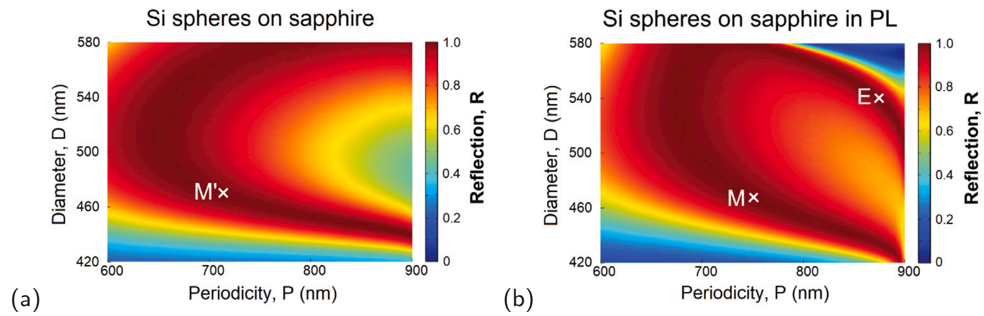

Fig. 2. Intensity reflection coefficients of metasurface calculated as a function of the nanoparticle diameter (D) and its periodicity (P). (a) Si spheres are placed on a sapphire substrate without a protective layer. (b) Si spheres are placed on a sapphire substrate and embedded in a protective layer with the refractive index $n_{PL} = 1.4$. The structure is irradiated by a plane monochromatic wave at normal angle of incidence. The marked points M'×, M× and E× indicate the parameters (D, P) for the structures discussed in the text below.

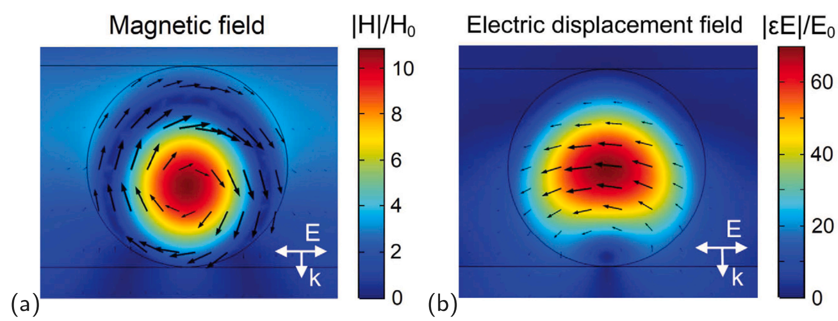

Fig. 3. Color map of (a) magnetic field distribution for M× point with $D = 468$ nm; $P = 750$ nm and (b) electric displacement field for E× point with $D = 540$ nm; $P = 874$ nm, normalized at the values of the magnetic H_0 and electric E_0 fields of the incident plane wave, respectively. Direction and magnitude of the electric current densities are shown by black arrows in both images.

maximum value of the period variation should be smaller than 885 nm (λ/n_{sub}) to exclude diffraction effects into the sapphire substrate [36]. The dark red zone corresponds to a reflection of almost 100%. From a comparison of the results in Fig. 2a and Fig. 2b, it can be seen that the inclusion of the protective layer leads only to a shift of the zone with maximum (~ 100%) reflection (dark red areas) with regard to the design parameters (diameter and periodicity).

To elucidate the physical cause of almost ideal reflection, let us consider the field distributions in metasurface nanoparticles for cases when the reflection coefficient approaches 1. Fig. 3 presents the magnetic (a) and electric (b) fields inside Si nanoparticles calculated for the parameters corresponding to the marked points M× and E× in Fig. 2b, respectively. For the point M×, the strong magnetic field is generated at the center of the Si nanoparticles (Fig. 3a), while for the other point E×, we observe at the center the strong electric displacement field (Fig. 3b). Note that such field distributions correspond to the magnetic and electric dipole resonant responses [37], respectively. Thus, we can conclude that almost ideal reflection is realized due to the resonant excitation of magnetic or electric dipole moments of Si nanoparticles. At these conditions every nanoparticle of the metasurface generates strong secondary waves which destructively interfere with incident waves in the transmission direction resulting in the suppression of total transmission and the realization of a perfect metamirror.

It is important to note that in the case of a homogeneous environment, perfect reflection can also be obtained due to resonant excitation of a certain multipole moment of metasurface nanoparticles (a detailed discussion of this question may be found elsewhere [38]). In our previous paper [19], the perfect reflection effect in the framework of the coupled dipole approximation (CDA) has been theoretically proven. In the CDA approach the reflection R and transmission T coefficients of a metasurface located in a homogeneous medium and composed of dipole nanospheres are determined by the nanosphere effective magnetic α_m^{eff} and electric α_p^{eff} dipole polarizabilities [39]

$$R = \frac{k_d^2}{4S_L^2}\left([\mathrm{Re}(\alpha_p^{eff}) - \mathrm{Re}(\alpha_m^{eff})]^2 + [\mathrm{Im}(\alpha_p^{eff}) - \mathrm{Im}(\alpha_m^{eff})]^2\right), \quad (1)$$

$$T = \left(1 - \frac{k_d}{2S_L}[\mathrm{Im}(\alpha_p^{eff}) + \mathrm{Im}(\alpha_m^{eff})]\right)^2 + \frac{k_d^2}{4S_L^2}[\mathrm{Re}(\alpha_p^{eff}) - \mathrm{Re}(\alpha_m^{eff})]^2, \quad (2)$$

where k_d is the wave number in the surrounding medium, $S_L = P^2$ is the elementary cell area defined as a square of periodicity. In [18,19], using Eqs. (1) and (2), it has been demonstrated that perfect reflection can be reached at the electric or magnetic dipole resonances.

The presence of the sapphire substrate and the protective layer do not prevent the realization of perfect reflection due to the magnetic or electric dipole resonances of Si nanospheres. The existence of the sapphire substrate results in modification of the dimensional parameters (compared to the case of a homogeneous environment) corresponding to ideal reflection. A more thorough analysis of a multi-layer medium with different refractive indices will be considered in the next section.

3. Results and discussion

3.1. Substrate and embedding layer impact

First, we consider a model when the particles are located in air and placed on dielectric substrates with different refractive indices (RI). At the condition of the magnetic dipole resonance marked as the point M'× in Fig. 2a, the changes of the substrate RI within the range from 1.65 to 1.85 do not affect the optimal metasurface period for perfect reflection (Fig. 4a). Substrates with higher refractive indices are not considered in this paper in order to exclude a discussion of diffraction effects introduced by the substrate material.

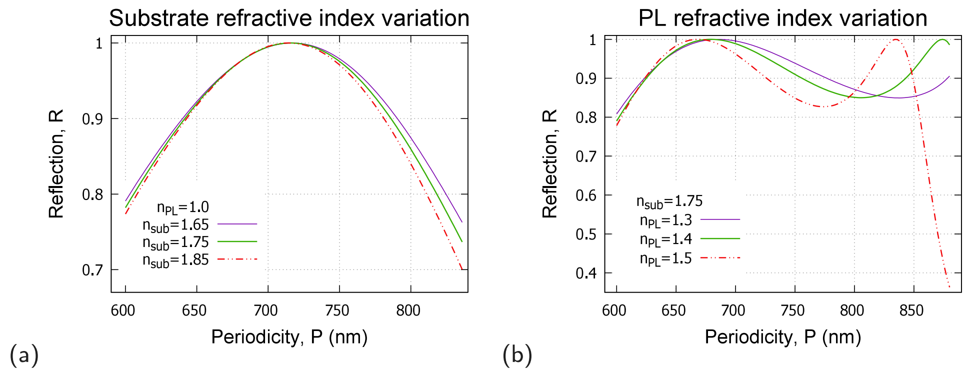

Fig. 4. (a) Influence of the substrate refractive index on the reflectivity of the metamirror. The diameter of nanoparticles is fixed at $D = 468$ nm (marked as M'× in Fig. 2a). (b) The dependence of power reflection coefficients on the periodicity for different refractive indices of the protective layer (PL) for the nanoparticle diameter $D = 540$ nm. The left and right peaks correspond to the magnetic and electric resonances, correspondingly (the latter is labeled as E× in Fig. 2b).

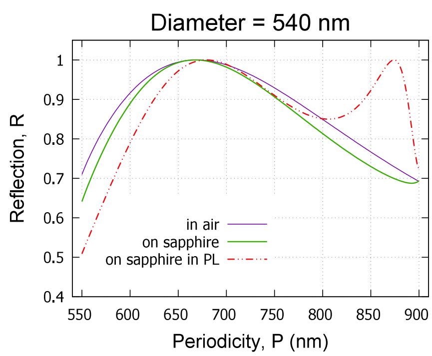

Fig. 5. Influence of the environment on the metamirror reflection for the fixed nanoparticle diameter $D = 540$ nm: nanoparticles in air (purple), placed on a sapphire substrate (green), and additionally embedded in a protective layer with refractive index $n_{PL} = 1.4$ (red).

When the particles are placed on a sapphire substrate ($n_{sub} = 1.75$) and additionally embedded in a protective layer, the sets of dimensional parameters like nanoparticle diameter and periodicity required for the realization of high reflectivity tend to be altered (see Fig. 2b). The magnetic dipole resonance is less affected by presence of the protective layer (see the perfect reflection around $P = 670$ nm in Fig. 4b), since in this case the strong magnetic field is confined inside the nanoparticles. Conversely, the electric dipole resonance depends higher on the refractive index of the surrounding material, due to the strong electric near-field interaction in the metasurface. For periodicity around $P = 850$ nm in Fig. 4b, one can see that the peak of the electric dipole resonance is strongly shifted to lower periodicity for higher refractive index of the protective layer, because with increasing refractive index the distance between the nanospheres providing the same interaction force is decreased.

Comparison of reflectances for metasurfaces in three different environments is shown in Fig. 5. The configuration when an array of silicon nanoparticles is placed on a sapphire substrate and enclosed in a protective layer (red line) has two peaks corresponding to perfect reflection. The right peak at the periodicity of 874 nm is formed by the excitation of electric dipole moment. It appears due to the strong shift of the electric dipole resonance when the protective layer is included. The left peak corresponds to the magnetic dipole resonance and observed also in the configurations when the environment is simplified to a homogeneous medium, like air, or nanospheres are placed on a sapphire substrate without a protective layer.

3.2. Analysis of imperfections

The computational accuracy allows to define how precise we can estimate the optical properties and their changes due to configuration or parameter uncertainties related to the fabrication of the metasurface and other devices [40]. The accuracy of the conducted simulations reaches 10^{-5} using a mathematical approach called Perfectly Matched Layer (PML). The PML boundary condition allows to avoid back reflection from the computational boundary of the model and not to interfere with the originally scattered field. Therefore, the limiting computational error is related to the model discretization that depends on the computational time and resources.

The fabricated metasurface will not consist of perfectly identical nanoparticles separated at perfectly identical distance from each other. Such parameters as the diameter and periodicity can fluctuate in a certain range defined by the accuracy and precision of the fabrication technology. To estimate the intensity reflection changes in case of imperfections, we explicitly consider elementary cells with $2{\times}2 = 4$ and $3 \times 3 = 9$ nanoparticles and randomize their parameters around corresponding perfect values in the simulation of the metasurface reflection properties (see Fig. 6a,b). We consider the case of perfect reflection at the following parameters ($D = 476$ nm, $P = 730$ nm) of the infinite metasurface structure on a sapphire substrate embedded in a protective layer with the refractive index $n_{PL} = 1.4$ (Fig. 2b). These parameters are chosen to provide a relatively broadband mirror performance, expected from a broad red zone of high reflection in Fig. 2b. Moreover, the distance between the nanoparticles is large enough to avoid their contact. That makes this set of parameters feasible in the fabrication process.

We conducted 100 simulations for different random configurations and calculated the mean value of the reflection coefficients. The standard errors of the mean for all solutions are also presented in Fig. 6. The fluctuations of nanoparticle diameters (Fig. 6a) decrease the mean value of the reflection coefficient more significantly than the fluctuations of periodicity (Fig. 6b). When diameters differ from the perfect value by less than 6%, the structure can still be considered as a highly-efficient mirror.

The metasurface is embedded in a thin layer to protect the structure against possible damage and impurities. However, the thickness of the protective layer may also have fluctuations. Driven by the question if the accuracy of the layer deposition would be relevant in future experiments, we analyzed changes of the intensity reflection coefficients for different protective layer thicknesses considering two cases presented in Fig. 7. The red curve corresponds to the resonant excitation of electric dipole moments ($D = 540$ nm; $P = 874$ nm). The blue curve corresponds to the magnetic resonant response ($D = 480$ nm; $P = 722$ nm). The dimensional parameters of Si nanospheres in both cases are taken at the conditions of perfect reflection when the thickness of

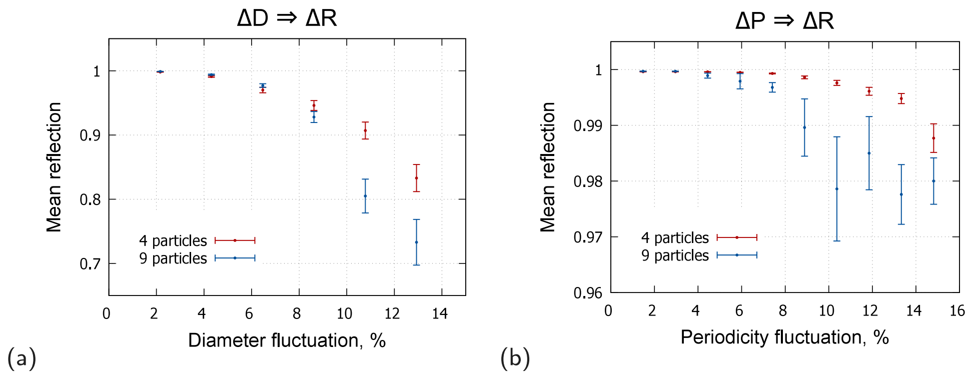

Fig. 6. The influence of (a) nanoparticle diameter fluctuations and (b) periodicity fluctuations on the mean value of power reflection coefficient. We consider the case of perfect reflection at the following parameters ($D = 476$ nm, $P = 730$ nm) of the infinite metasurface structure located on a substrate and embedded in a protective layer. Refractive indices of the substrate and protective layer are $n_{sub} = 1.75$ and $n_{PL} = 1.4$, respectively.

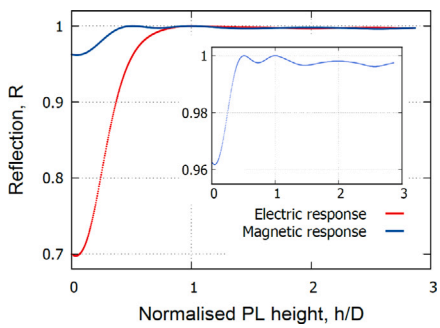

Fig. 7. Power reflection coefficients of metasurface calculated as a function of the protective layer thickness, normalized to the value of the nanoparticle diameter (h/D). The simulations are run at the conditions of magnetic and electric dipole resonances.

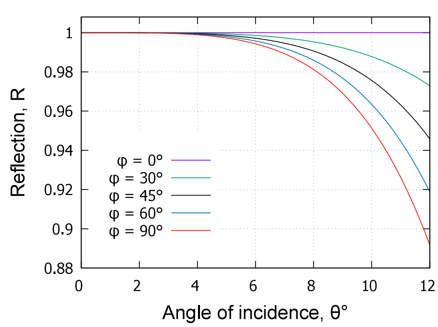

Fig. 8. Tolerable angle of incidence θ of the light beam for different polarization angles φ: $\varphi = 0°$ ($\varphi = 90°$) corresponds to s- (p-) polarization of the electric field. The parameters of metasurface: $D = 468$ nm, $P = 750$ nm. Refractive index of the substrate $n_{sub} = 1.75$, of the protective layer $n_{PL} = 1.4$.

the protective layer is equal to the nanoparticle diameter. Fluctuations in the layer thickness does not significantly decrease the intensity reflection. When the layer thickness is smaller than the nanoparticle diameter, the electric dipole moments change and a reduction of reflectivity is observed, since near-field interactions between electric dipole moments are sensitive to the surrounding medium. The magnetic dipole resonance is less sensitive due to the localization of the electric field inside the nanoparticles.

We consider now the case of a slightly oblique incidence of light on the metasurface and introduce in addition a polarization angle φ. Here the angle $\varphi = 0°$ ($\varphi = 90°$) corresponds to s-polarized (p-polarized) light with $\mathbf{E}_0$ perpendicular (parallel) to the plane of incidence (yz-plane in Fig. 1). The dependence of the intensity reflection coefficient on the angle of incidence and the polarization angle are illustrated in Fig. 8. The investigated point is chosen for the magnetic dipole resonance ($D = 468$ nm, $P = 750$ nm) marked as M× in Fig. 2b. The metasurface remains highly-reflective for all polarizations of the electric field if the angle of incidence is less than 4°. Note, that for the s-polarization the reflection remains higher than 0.999 up to 20°.

4. Conclusion

This article reports on our ongoing work towards the realization of a highly efficient silicon nanosphere metasurface mirror. The metasurface consists of silicon nanoparticles located on a sapphire substrate and embedded in a protective layer. It has been demonstrated that the optical behavior of the metasurface mirror can be described by resonant excitation of electric and magnetic dipole moments. While the substrate does not noticeably affect the metasurface reflectivity, the presence of a protective layer requires adjustment of the size parameters (diameter and periodicity) of Si nanospheres at which perfect reflection is realized. Taking into account the role of possible metasurface imperfections, it has been found that fluctuations in the nanoparticle diameter have larger influence on the metasurface reflection compared to fluctuations in periodicity. If the diameter fluctuations are larger than 6% of the ideal value, the mirror effect may be significantly reduced. It has been demonstrated that the uncertainties in the thickness of the protective layer are not critical for the realization of a perfect mirror. As a final step, deviations in the angle of incidence were considered, showing that the ideal reflection is maintained at normal incidence and at angles of incidence less than 4 degrees for all polarization directions of the incident electric field.

Funding

Deutsche Forschungsgemeinschaft (DFG), Germany (EXC 2122, Project ID 390833453) and (EXC 2123, Project ID 390837967), Villum Fonden, Denmark (Grant No. 40707).

CRediT authorship contribution statement

Mariia Matiushechkina: Writing – original paper, Numerical simulations. **Andrey B. Evlyukhin:** Methodology, Paper preparation. **Vladimir A. Zenin:** Numerical simulations, Paper preparation. **Michèle Heurs:** Supervision, Conceptualization. **Boris N. Chichkov:** Coordination, Paper preparation.

Declaration of competing interest

The authors declare that they have no known competing financial interests or personal relationships that could have appeared to influence the work reported in this paper.

Data availability

Data will be made available on request.

Acknowledgments

Authors acknowledge financial support from the Deutsche Forschungsgemeinschaft, Germany (DFG, German Research Foundation) under Germany's Excellence Strategy within the Cluster of Excellence PhoenixD (EXC 2122, Project ID 390833453) and the Cluster of Excellence QuantumFrontiers (EXC 2123, Project ID 390837967).V.A.Z. acknowledges financial support from Villum Fonden, Denmark (Grant No. 40707).

References

[1] I. Staude, J. Schilling, Metamaterial-inspired silicon nanophotonics, Nat. Photon. 11 (5) (2017) 274–284, http://dx.doi.org/10.1038/nphoton.2017.39.

[2] R.S. Savelev, O.N. Sergaeva, D.G. Baranov, A.E. Krasnok, A. Alù, Dynamically reconfigurable metal-semiconductor Yagi-Uda nanoantenna, Phys. Rev. B 95 (2017) 235409, http://dx.doi.org/10.1103/PhysRevB.95.235409, URL https://link.aps.org/doi/10.1103/PhysRevB.95.235409.

[3] X. Zhu, W. Yan, U. Levy, N.A. Mortensen, A. Kristensen, Resonant laser printing of structural colors on high-index dielectric metasurfaces, Sci. Adv. 3 (5) (2017) e1602487, http://dx.doi.org/10.1126/sciadv.1602487, arXiv:https://www.science.org/doi/pdf/10.1126/sciadv.1602487.

[4] F. Zhang, M. Pu, X. Li, X. Ma, Y. Guo, P. Gao, H. Yu, M. Gu, X. Luo, Extreme-angle silicon infrared optics enabled by streamlined surfaces, Adv. Mater. 33 (11) (2021) 2008157, http://dx.doi.org/10.1002/adma.202008157, arXiv:https://onlinelibrary.wiley.com/doi/pdf/10.1002/adma.202008157.

[5] A.B. Evlyukhin, S.M. Novikov, U. Zywietz, R.L. Eriksen, C. Reinhardt, S.I. Bozhevolnyi, B.N. Chichkov, Demonstration of magnetic dipole resonances of dielectric nanospheres in the visible region, Nano Lett. 12 (7) (2012) 3749–3755, http://dx.doi.org/10.1021/nl301594s, PMID: 22703443.

[6] P. Spinelli, M.A. Verschuuren, A. Polman, Broadband omnidirectional antireflection coating based on subwavelength surface mie resonators, Nature Commun. 3 (1) (2012) 692, http://dx.doi.org/10.1038/ncomms1691.

[7] K.V. Baryshnikova, M.I. Petrov, V.E. Babicheva, P.A. Belov, Plasmonic and silicon spherical nanoparticle antireflective coatings, Sci. Rep. 6 (1) (2016) 22136, http://dx.doi.org/10.1038/srep22136.

[8] M. Pu, Y. Guo, X. Li, X. Ma, X. Luo, Revisitation of extraordinary Young's interference: from catenary optical fields to spin–orbit interaction in metasurfaces, ACS Photon. 5 (8) (2018) 3198–3204, http://dx.doi.org/10.1021/acsphotonics.8b00437.

[9] M. Decker, I. Staude, M. Falkner, J. Dominguez, D.N. Neshev, I. Brener, T. Pertsch, Y.S. Kivshar, High-efficiency dielectric huygens' surfaces, Adv. Opt. Mater. 3 (6) (2015) 813–820, http://dx.doi.org/10.1002/adom.201400584, arXiv:https://onlinelibrary.wiley.com/doi/pdf/10.1002/adom.201400584.

[10] A. Howes, W. Wang, I. Kravchenko, J. Valentine, Dynamic transmission control based on all-dielectric huygens metasurfaces, Optica 5 (7) (2018) 787–792, http://dx.doi.org/10.1364/OPTICA.5.000787, URL https://opg.optica.org/optica/abstract.cfm?URI=optica-5-7-787.

[11] V.E. Babicheva, A.B. Evlyukhin, Resonant lattice kerker effect in metasurfaces with electric and magnetic optical responses, Laser Photonics Rev. 11 (6) (2017) 1700132, http://dx.doi.org/10.1002/lpor.201700132, arXiv:https://onlinelibrary.wiley.com/doi/pdf/10.1002/lpor.201700132.

[12] P. Moitra, B.A. Slovick, W. li, I.I. Kravchencko, D.P. Briggs, S. Krishnamurthy, J. Valentine, Large-scale all-dielectric metamaterial perfect reflectors, ACS Photon. 2 (6) (2015) 692–698, http://dx.doi.org/10.1021/acsphotonics.5b00148.

[13] S. Taravati, G.V. Eleftheriades, Full-duplex reflective beamsteering metasurface featuring magnetless nonreciprocal amplification, Nature Commun. 12 (1) (2021) 4414, http://dx.doi.org/10.1038/s41467-021-24749-7.

[14] J. Martínez-Llinàs, C. Henry, D. Andrén, R. Verre, M. Käll, P. Tassin, A Gaussian reflective metasurface for advanced wavefront manipulation, Opt. Express 27 (15) (2019) 21069–21082, http://dx.doi.org/10.1364/OE.27.021069, URL https://opg.optica.org/oe/abstract.cfm?URI=oe-27-15-21069.

[15] G. Ding, K. Chen, X. Luo, G. Qian, J. Zhao, T. Jiang, Y. Feng, Direct routing of intensity-editable multi-beams by dual geometric phase interference in metasurface, Nanophotonics 9 (9) (2020) 2977–2987, http://dx.doi.org/10.1515/nanoph-2020-0203.

[16] H. Liu, H. Xue, Y. Liu, L. Li, Generation of multiple pseudo bessel beams with accurately controllable propagation directions and high efficiency using a reflective metasurface, Appl. Sci. 10 (20) (2020) 7219, http://dx.doi.org/10.3390/app10207219.

[17] B. Slovick, Z.G. Yu, M. Berding, S. Krishnamurthy, Perfect dielectric-metamaterial reflector, Phys. Rev. B 88 (2013) 165116, http://dx.doi.org/10.1103/PhysRevB.88.165116, URL https://link.aps.org/doi/10.1103/PhysRevB.88.165116.

[18] V.E. Babicheva, A.B. Evlyukhin, Resonant suppression of light transmission in high-refractive-index nanoparticle metasurfaces, Opt. Lett. 43 (21) (2018) 5186–5189, http://dx.doi.org/10.1364/OL.43.005186, URL https://opg.optica.org/ol/abstract.cfm?URI=ol-43-21-5186.

[19] A.B. Evlyukhin, M. Matiushechkina, V.A. Zenin, M. Heurs, B.N. Chichkov, Lightweight metasurface mirror of silicon nanospheres, [Invited], Opt. Mater. Express 10 (10) (2020) 2706–2716, http://dx.doi.org/10.1364/OME.409311, URL https://opg.optica.org/ome/abstract.cfm?URI=ome-10-10-2706.

[20] P. Cencillo-Abad, J.-Y. Ou, E. Plum, N.I. Zheludev, Electro-mechanical light modulator based on controlling the interaction of light with a metasurface, Sci. Rep. 7 (1) (2017) 5405, http://dx.doi.org/10.1038/s41598-017-05906-9.

[21] C.A. Curwen, J.L. Reno, B.S. Williams, Broadband continuous single-mode tuning of a short-cavity quantum-cascade VECSEL, Nat. Photon. 13 (12) (2019) 855–859, http://dx.doi.org/10.1038/s41566-019-0518-z.

[22] J. Li, J. Li, S. Zhou, F. Yi, Metasurface photodetectors, Micromachines 12 (12) (2021) http://dx.doi.org/10.3390/mi12121584, URL https://www.mdpi.com/2072-666X/12/12/1584.

[23] R.X. Adhikari, K. Arai, A.F. Brooks, et al., A cryogenic silicon interferometer for gravitational-wave detection, Classical Quantum Gravity 37 (16) (2020) 165003, http://dx.doi.org/10.1088/1361-6382/ab9143.

[24] M. Punturo, H. Lück, Toward a third generation of gravitational wave observatories, Gen. Relativity Gravitation 43 (2) (2011) 363–385, http://dx.doi.org/10.1007/s10714-010-1010-8.

[25] E. Hirose, K. Craig, H. Ishitsuka, I.W. Martin, N. Mio, S. Moriwaki, P.G. Murray, M. Ohashi, S. Rowan, Y. Sakakibara, T. Suzuki, K. Waseda, K. Watanabe, K. Yamamoto, Mechanical loss of a multilayer tantala/silica coating on a sapphire disk at cryogenic temperatures: Toward the KAGRA gravitational wave detector, Phys. Rev. D 90 (2014) 102004, http://dx.doi.org/10.1103/PhysRevD.90.102004, URL https://link.aps.org/doi/10.1103/PhysRevD.90.102004.

[26] S. Reid, I.W. Martin, Development of mirror coatings for gravitational wave detectors, Coatings 6 (4) (2016) http://dx.doi.org/10.3390/coatings6040061, URL https://www.mdpi.com/2079-6412/6/4/61.

[27] J. Steinlechner, I.W. Martin, A.S. Bell, J. Hough, M. Fletcher, P.G. Murray, R. Robie, S. Rowan, R. Schnabel, Silicon-based optical mirror coatings for ultrahigh precision metrology and sensing, Phys. Rev. Lett. 120 (2018) 263602, http://dx.doi.org/10.1103/PhysRevLett.120.263602, URL https://link.aps.org/doi/10.1103/PhysRevLett.120.263602.

[28] F. Moreno, B. García-Cámara, J.M. Saiz, F. González, Interaction of nanoparticles with substrates: effects on the dipolar behaviour of the particles, Opt. Express 16 (17) (2008) 12487–12504, http://dx.doi.org/10.1364/OE.16.012487, URL https://opg.optica.org/oe/abstract.cfm?URI=oe-16-17-12487.

[29] N.L.D. Serhiy Z. Malynych, I.E. Moroz, Influence of substrate on the optical properties of non-aggregated silver nanoparticles, Eur. Phys. J. Appl. Phys. 2 (64) (2013) 20402, http://dx.doi.org/10.1051/epjap/2013120531.

[30] A.E. Miroshnichenko, A.B. Evlyukhin, Y.S. Kivshar, B.N. Chichkov, Substrate-induced resonant magnetoelectric effects for dielectric nanoparticles, ACS Photon. 2 (10) (2015) 1423–1428, http://dx.doi.org/10.1021/acsphotonics.5b00117.

[31] M. Hesari-Shermeh, B. Abbasi-Arand, M. Yazdi, Analysis of substrated periodic metasurfaces under normal incidence, Opt. Express 29 (2) (2021) 1694–1710, http://dx.doi.org/10.1364/OE.413103, URL https://opg.optica.org/oe/abstract.cfm?URI=oe-29-2-1694.

[32] J. van de Groep, A. Polman, Designing dielectric resonators on substrates: Combining magnetic and electric resonances, Opt. Express 21 (22) (2013) 26285–26302, http://dx.doi.org/10.1364/OE.21.026285, URL https://opg.optica.org/oe/abstract.cfm?URI=oe-21-22-26285.

[33] S. Rowan, G. Cagnoli, P. Sneddon, J. Hough, R. Route, E. Gustafson, M. Fejer, V. Mitrofanov, Investigation of mechanical loss factors of some candidate materials for the test masses of gravitational wave detectors, Phys. Lett. A 265 (1) (2000) 5–11, http://dx.doi.org/10.1016/S0375-9601(99)00874-9, URL https://www.sciencedirect.com/science/article/pii/S0375960199008749.

[34] S. Reid, G. Cagnoli, D. Crooks, J. Hough, P. Murray, S. Rowan, M. Fejer, R. Route, S. Zappe, Mechanical dissipation in silicon flexures, Phys. Lett. A 351 (4) (2006) 205–211, http://dx.doi.org/10.1016/j.physleta.2005.10.103, URL https://www.sciencedirect.com/science/article/pii/S0375960105016981.

[35] D.R.H. Craig F. Bohren, Absorption and scattering of light by small particles, ISBN: 9783527618156, 1998, http://dx.doi.org/10.1002/9783527618156.ch1, arXiv:https://onlinelibrary.wiley.com/doi/pdf/10.1002/9783527618156.ch1.

[36] V.G. Kravets, F. Schedin, A.N. Grigorenko, Extremely narrow plasmon resonances based on diffraction coupling of localized plasmons in arrays of metallic nanoparticles, Phys. Rev. Lett. 101 (2008) 087403, http://dx.doi.org/10.1103/PhysRevLett.101.087403, URL https://link.aps.org/doi/10.1103/PhysRevLett.101.087403.

[37] U. Zywietz, A.B. Evlyukhin, C. Reinhardt, B.N. Chichkov, Laser printing of silicon nanoparticles with resonant optical electric and magnetic responses, Nature Commun. 5 (1) (2014) 3402, http://dx.doi.org/10.1038/ncomms4402.

[38] V.E. Babicheva, A.B. Evlyukhin, Multipole lattice effects in high refractive index metasurfaces, J. Appl. Phys. 129 (4) (2021) 040902, http://dx.doi.org/10.1063/5.0024274.

[39] A.B. Evlyukhin, C. Reinhardt, A. Seidel, B.S. Luk'yanchuk, B.N. Chichkov, Optical response features of Si-nanoparticle arrays, Phys. Rev. B 82 (2010) 045404, http://dx.doi.org/10.1103/PhysRevB.82.045404, URL https://link.aps.org/doi/10.1103/PhysRevB.82.045404.

[40] S.N. Khonina, N.L. Kazanskiy, M.A. Butt, S.V. Karpeev, Optical multiplexing techniques and their marriage for on-chip and optical fiber communication: a review, Opto-Electron. Adv. 5 (8) (2022) 210127–1–210127–25, http://dx.doi.org/10.29026/oea.2022.210127, URL http://www.chinaoceanengin.cn//article/id/62cfc87b99d88171c95f55bd.